The EMBO Journal vol.14 no.19 pp.4883–4892, 1995

Two distinct recognition signals define the site of endonucleolytic cleavage at the 5′-end of yeast 18S rRNA

Jaap Venema, Yves Henry[1] and David Tollervey[2]

EMBL, Gene Expression Programme, Postfach 10.2209, 69012 Heidelberg, Germany
[1]Present address: Institut de Biologie Cellulaire et de Génétique du CNRS, LBME, 118 Route de Narbonne, 31062 Toulouse Cedex, France

[2]Corresponding author

Three of the four eukaryotic ribosomal RNA molecules (18S, 5.8S and 25–28S rRNA) are transcribed as a single precursor, which is subsequently processed into the mature species by a complex series of cleavage and modification reactions. Early cleavage at site A1 generates the mature 5′-end of 18S rRNA. Mutational analyses have identified a number of upstream regions in the 5′ external transcribed spacer (5′ ETS), including a U3 binding site, which are required *in cis* for processing at A1. Nothing is known, however, about the requirement for *cis*-acting elements which define the position of the 5′-end of the 18S rRNA or of any other eukaryotic rRNA. We have introduced mutations around A1 and analysed them *in vivo* in a genetic background where the mutant pre-rRNA is the only species synthesized. The results indicate that the mature 5′-end of 18S rRNA in yeast is identified by two partially independent recognition systems, both defining the same cleavage site. One mechanism identifies the site of cleavage at A1 in a sequence-specific manner involving recognition of phylogenetically conserved nucleotides immediately upstream of A1 in the 5′ ETS. The second mechanism specifies the 5′-end of 18S rRNA by spacing the A1 cleavage at a fixed distance of 3 nt from the 5′ stem–loop/pseudoknot structure located within the mature sequence. The 5′ product of the A1 processing reaction can also be identified, showing that, in contrast to yeast 5.8S rRNA, the 5′-end of 18S rRNA is generated by endonucleolytic cleavage.

Keywords: endonuclease/RNA processing/ribosomal RNA/ribosome/*Saccharomyces cerevisiae*

Introduction

Pre-rRNA processing in eukaryotic cells comprises a complex series of reactions leading from a single precursor to the mature 18S, 5.8S and 25–28S rRNA molecules. The primary precursor contains, in addition to the mature rRNA species, two external transcribed spacers at its 5′ and 3′-ends (5′ ETS and 3′ ETS respectively), as well as two internal transcribed spacers (ITS1 and ITS2; see Figure 1). After synthesis of the primary pre-rRNA molecule by RNA polymerase I is completed the transcribed spacer sequences are removed by a series of endonucleolytic cleavages and exonucleolytic degradation steps (Eichler and Craig, 1994). In addition, the pre-rRNA undergoes modification by pseudo-uridinylation and methylation at many different sites (Klootwijk and Planta, 1989). The processing pathway is best characterized in the yeast *Saccharomyces cerevisiae* (see Figure 1). In this organism the primary 35S precursor is first cleaved at site A0 in the 5′ ETS (Hughes and Ares, 1991), immediately followed by processing at sites A1, the 5′-end of the mature 18S rRNA, and A2 in ITS1. This yields the 20S precursor, which is subsequently converted into mature 18S rRNA by cleavage at its 3′-end (site D); this is reported to be a cytoplasmic event occurring at a late stage in the pathway (Udem and Warner, 1973; Veldman *et al.*, 1980). The remaining 3′ part of the molecule, $27SA_2$ pre-rRNA, is subsequently processed to 5.8S and 25S rRNAs by one of two alternative processing pathways in ITS1 (Henry *et al.*, 1994).

Genetic analysis in yeast has resulted in the identification of a large number of *trans*-acting factors involved in pre-rRNA processing. The most important class is formed by the small nucleolar ribonucleoprotein particles (snoRNPs), consisting of snoRNA molecules associated with different proteins. Three snoRNAs (U3, U14 and snR30) have been shown to be essential for synthesis of 18S rRNA, whereas synthesis of 25S and 5.8S rRNA remains unaffected in cells genetically depleted of these components (Li *et al.*, 1990; Hughes and Ares, 1991; Morrissey and Tollervey, 1993). In addition to the snoRNA molecules, several snoRNP protein components, including Nop1p, Sof1p and Gar1p, are also required for 18S rRNA synthesis (Tollervey *et al.*, 1991; Girard *et al.*, 1992; Jansen *et al.*, 1993). Interestingly, loss of 18S rRNA synthesis due to inactivation of any one of these *trans*-acting factors appears to be the result of a common phenotype, i.e. inhibition of cleavage at processing sites A1 and A2. Depletion of U3 or its associated proteins Nop1p and Sof1p also inhibits processing at A0, in addition to A1 and A2 (Beltrame *et al.*, 1994). U3 is one of the most extensively studied snoRNPs and in yeast it has recently been shown to operate, at least partly, by direct base pairing of its RNA moiety with a 10 nucleotide (nt) sequence in the 5′ ETS (Beltrame and Tollervey, 1992; Beltrame *et al.*, 1994). Genetic depletion *in trans* of the U3 snoRNA or deletion *in cis* of the 5′ ETS sequence element both result in the phenotype described above (Beltrame *et al.*, 1994). The U3 complementary sequence in the 5′ ETS is therefore essential for cleavages which occur more than 100 (A0), 200 (A1) and 2000 (A2) nt further downstream. Similarly, an early processing event in the metazoan 5′ ETS has been found to be dependent on U3 (Kass *et al.*, 1990; Mougey *et al.*, 1993). Furthermore, recent mutational analysis in yeast has produced evidence for additional

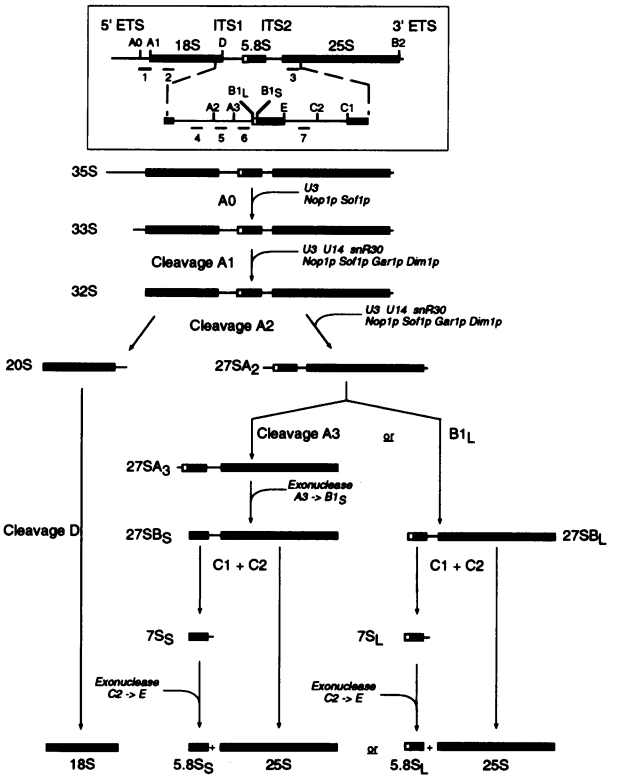

Fig. 1. Structure and processing of pre-rRNA in *Saccharomyces cerevisiae*. The boxed area shows the 35S pre-rRNA and the location of the various oligonucleotides (numbered 2–7) used in this study. Oligonucleotides 2 and 3 are complementary to the tags in the 18S and 25S rRNA genes respectively. Probe 1 is a riboprobe complementary to the region between A0 and A1 in the 5′ ETS. Bars represent mature rRNA sequences, thin lines represent transcribed spacers. Processing of the primary 35S precursor starts at A0, yielding 33S pre-rRNA. This molecule is then subsequently processed at sites A1 and A2, giving rise to the 20S and $27SA_2$ precursors. Cleavage at A2 separates the pre-rRNAs destined for the small and large ribosomal subunit. The 20S precursor is then endonucleolytically cleaved at site D, to yield the mature 18S rRNA. The $27SA_2$ precursor is processed by two alternative pathways, forming the mature 5.8S and 25S rRNAs. Processing step B2 at the 3′-end of 25S rRNA, the timing of which is unclear, is not shown in this pathway. Direct cleavage of the 33S pre-rRNA at site A3 generates the aberrant 22S species described in this study, as well as $27SA_3$ pre-rRNA, which can be further processed to $5.8S_S$ and 25S rRNA. Note that the nomenclature for the 27SA pre-rRNAs differs slightly from that previously proposed (Henry *et al.*, 1994), i.e. 27SA and 27SA′ are now designated $27SA_2$ and $27SA_3$ respectively, pointing to their 5′-ends being A2 and A3. *Trans*-acting factors required for the different processing steps are indicated in italics. The role of the Dim1p protein in processing at A1 and A2 is from Lafontaine *et al.* (1995). The role of the exonuclease producing the 3′-end of 5.8S rRNA is from results obtained in our laboratory (P.Mitchell, E.Petfalski and D.Tollervey, unpublished data).

sequences in the 5′-terminal region of the 5′ ETS that are required *in cis* for synthesis of 18S rRNA (Van Nues *et al.*, 1995).

So far nothing is known about the mechanism by which the 5′-end of 18S rRNA is formed or about the requirement for sequences surrounding the A1 cleavage site. In *Escherichia coli* RNase III generates a 17S precursor by cleaving at both sides of a stem structure that is formed by sequences flanking the mature ends of the homologous 16S rRNA. The 17S pre-rRNA is subsequently converted into the mature 16S molecule by two as yet uncharacterized enzymatic activities (Srivastava and Schlessinger, 1990; Apirion and Miczak, 1993). The 5′-end of human 18S rRNA is reported to be formed *in vitro* by the activity of exonucleases from a precursor that is several nucleotides longer than the mature species (Hannon *et al.*, 1989; Yu and Nilsen, 1992). In this work we aimed to determine whether the 5′-end of yeast 18S rRNA is generated by direct endonucleolytic cleavage or by exonuclease digestion and to identify the *cis*-acting sequences which specify the position of the 5′-end of 18S rRNA. By introducing and analysing rRNA mutations in a genetic background where only mutant pre-rRNA is synthesized we found that the 5′-end of yeast 18S rRNA is in fact defined by two partly independent mechanisms, both specifying an endonucleolytic cleavage. One involves recognition of conserved 5′ ETS sequences upstream of A1, whereas a second mechanism operates from within 18S rRNA.

Results

Experimental system

Mutational analysis of *cis*-acting elements involved in A1 recognition was performed using yeast strain NOY504, which is temperature sensitive for RNA polymerase I transcription (Nogi *et al.*, 1993). This strain is complemented by a plasmid (pGAL::rDNA) which expresses the mutant pre-rRNA under control of the inducible GAL7 promoter (Henry *et al.*, 1994). Growth in galactose-based medium at the non-permissive temperature (37°C) results in loss of chromosomal rRNA synthesis and renders cell growth completely dependent on maturation of mutant pre-rRNA. The ability of the mutant pre-rRNA to support growth under these conditions is therefore a first indication of the severity of the effect of the mutation on rRNA synthesis. Furthermore, this system allows a detailed analysis of the effect of the mutation on pre-rRNA processing by Northern and primer extension analyses using probes recognizing sequences throughout the entire rDNA unit. After growth for 6 h at the non-permissive temperature chromosomal rRNA synthesis has dropped to $<10\%$ of the level of plasmid transcription and therefore virtually all of the newly synthesized pre-rRNA molecules are derived from the GAL7–rDNA units. The presence of small oligonucleotide tags in the mature 18S, 5.8S and 25S rRNA sequences further allows specific detection of the mature rRNAs transcribed from the plasmid (Henry *et al.*, 1994).

Effect of A1 mutations on 18S rRNA and A1 processing

In order to identify elements potentially involved in A1 processing the 5′ ETS sequences of various yeast species were determined and aligned to search for possible conserved motifs (Figure 2A). Despite very low overall conservation of primary sequence throughout most of the 5′ ETS (data not shown), the 6 nt immediately upstream of site A1 were found to be identical in these yeast species, although the evolutionarily distant *Schizosaccharomyces pombe* possesses an extra adenosine 5′ to A1 (Balzi *et al.*, 1985) (Figure 2A). To test their importance the evolutionarily conserved 6 nt were substituted, yielding mutant A1-Xho (Figure 2B). The importance of the sequence surrounding the A1 processing site itself was also assessed by substituting 4 nt across A1 (Figure 2B,

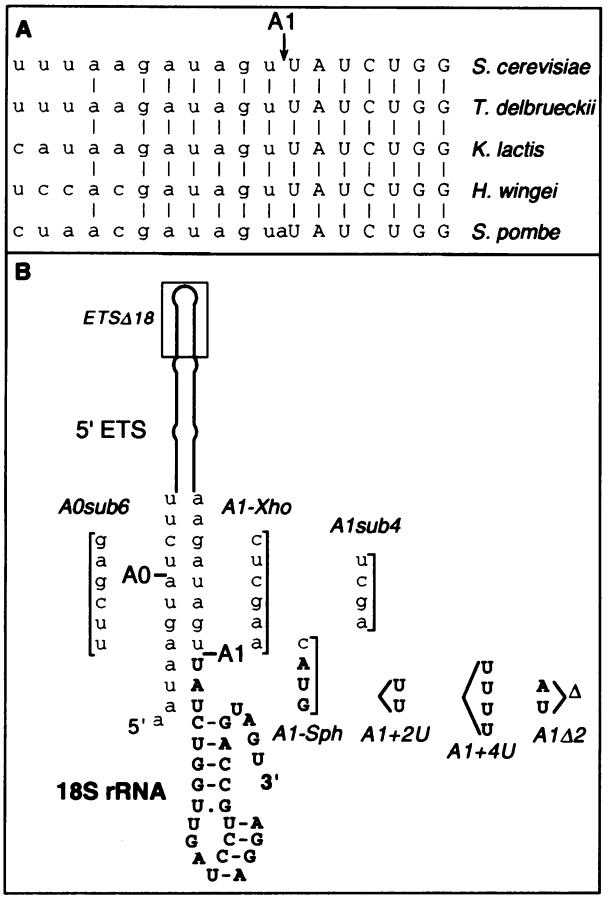

Fig. 2. Primary and secondary structure of the sequence surrounding A1. (**A**) Alignment of 5′ ETS (lower case) and 18S rRNA (upper case) sequences from different yeast species, shown in order of increasing evolutionary distance from *S.cerevisiae*. Data for *S.pombe* are from Balzi *et al.* (1985); the sequences for the other three species are unpublished (J.Venema and H.A.Raué) and have been deposited in the EMBL database under accession numbers X87400 (*Torulaspora delbrueckii*), X87402 (*Kluyveromyces lactis*) and X87403 (*Hansenula wingei*). In all cases the 5′-end of 18S rRNA and the first 6 nt in the 5′ ETS are identical, with the sole exception of an extra adenosine in the *S.pombe* sequence. Similar phylogenetic conservation is not observed between the spacers of distantly related vertebrate species. Conservation of primary sequence in the rest of the 5′ ETS is limited (data not shown). (**B**) Secondary structure of the region surrounding processing sites A0 and A1. Spacer nucleotides are shown in lower case, 18S rRNA sequences are in bold, upper case. The positions of the A0 and A1 cleavage sites are indicated. The structure of the schematically drawn stem–loop in the yeast 5′ ETS was taken from Yeh and Lee (1992). The exact structure of the sequences around A0 and A1 is unclear. The diagram depicts this region as single-stranded, but the potential exists for more extensive base pairing between the nucleotides on the left and right sides. The secondary structure of 18S rRNA is well established (Gutell *et al.*, 1994). The mutations analysed in this study are represented to the right, while two additional mutants for which data are not shown are drawn on the left. For simplicity the A1+2sub4 and A1Δ2sub4 mutations have not been drawn on the diagram; they consist of a combination of A1sub4 with the A1+2U and A1Δ2 mutations respectively. Note that due to a PCR error the A1-Xho mutation does not create an *Xho*I site as designed. For all mutants in this study the sequence of the cloned PCR fragment was fully verified by sequencing.

mutant A1-Sph) leading to an alteration of 3 nt at the 5′-end of the 18S rRNA.

Surprisingly, neither the A1-Xho nor the A1-Sph mutation affects growth on galactose plates at the non-permissive temperature (data not shown), indicating that

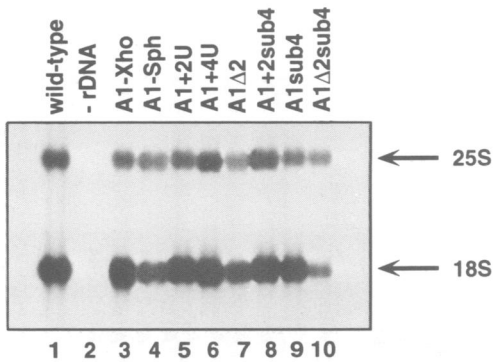

Fig. 3. Northern analysis of 18S and 25S rRNA in A1 mutants. RNA was extracted from NOY504 transformants expressing the mutant pre-rRNA following growth for 6 h at 37°C and analysed by Northern hybridization using the oligonucleotide tags in the 18S and 25S rRNA (numbered 2 and 3 in Figure 1). Lane 1, strain carrying the wild-type rDNA sequence. Lane 2, strain carrying a plasmid without rDNA sequences. Lane 3, strain carrying the A1-Xho mutation. Lane 4, A1-Sph. Lane 5, A1+2U. Lane 6, A1+4U. Lane 7, A1Δ2. Lane 8, A1+2sub4. Lane 9, A1sub4. Lane 10, A1Δ2sub4. The positions of the mature 18S and 25S rRNAs are indicated on the right.

the substituted nucleotides are not essential for synthesis of 18S rRNA. Moreover, the A1-Sph mutant, carrying the altered 5′-terminal 18S rRNA nucleotides, does not appear to be impaired in ribosomal function. To determine the effect of these mutations on the synthesis of 18S rRNA total RNA was isolated from transformants grown in synthetic galactose medium and shifted for 6 h to 37°C. The steady-state level of the mature rRNAs was determined by Northern analysis using the tags present in the 18S and 25S rRNA genes (corresponding to oligonucleotides 2 and 3 in Figure 1). The level of 25S rRNA was taken as an internal control, since it is unlikely to be affected by the small mutations around A1. The 18S rRNA level in the A1-Xho mutant (Figure 3, lane 3) is comparable with that in the wild-type control (Figure 3, lane 1), whereas the A1-Sph mutation mildly reduces accumulation of mature 18S rRNA (Figure 3, cf. lanes 1 and 4). Transformants carrying a plasmid without the GAL7–rDNA unit do not show any background signals (Figure 3, lane 2), indicating that only tagged, plasmid-derived 18S and 25S rRNAs are detected.

To analyse the accuracy and efficiency with which the 5′-end of 18S rRNA is formed primer extension was performed using the 18S rRNA tag, located 190 nt downstream in the mutant 18S rRNA gene. The 5′-end of 18S rRNA in the A1-Xho mutant (Figure 4A, lane 3) is formed at the wild-type position and with the same efficiency when compared with the wild-type rRNA (Figure 4A, lane 1). In accordance with the data from the Northern analysis, the intensity of the band due to A1 cleavage is somewhat lower in the A1-Sph mutant, but processing is accurate at the nucleotide level (Figure 4A, lane 4). The results of the primer extension experiments for these and all other A1 mutants are schematically summarized in Figure 5.

From these data we conclude that neither the primary sequence at the A1 site nor the phylogenetically conserved nucleotides immediately upstream are essential for A1 processing. Following these results, the only other candidate regions in the 5′ ETS for sequences that might

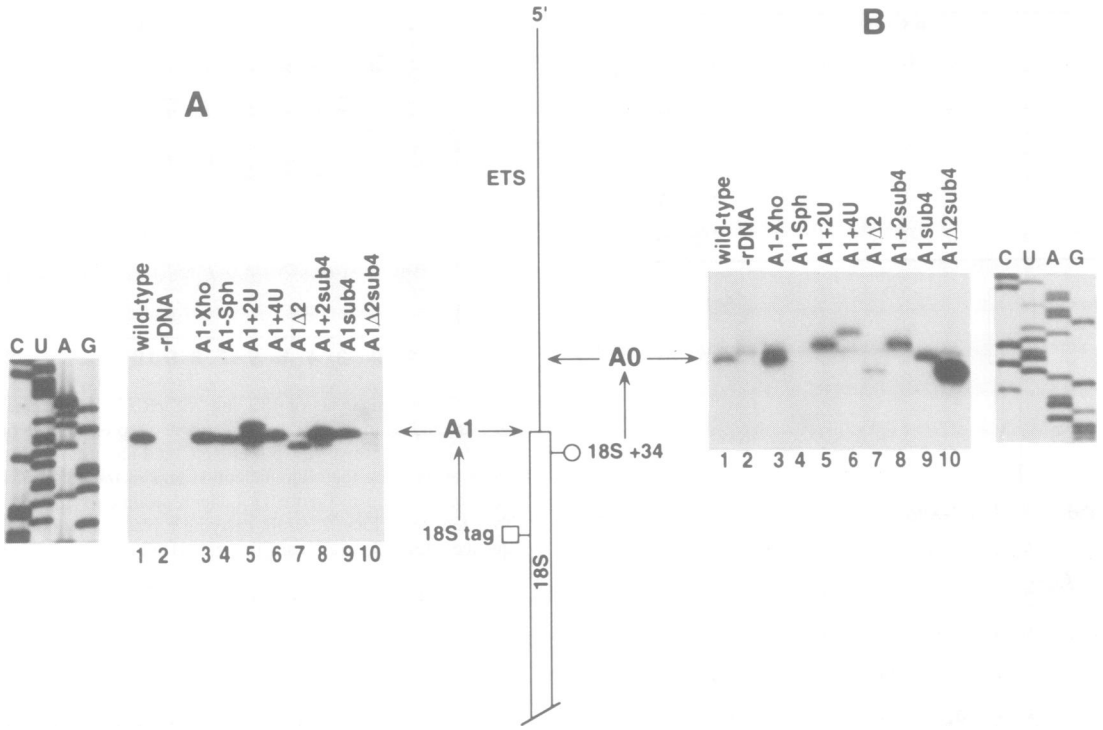

Fig. 4. Primer extension analysis of A1 mutants. RNA was extracted from NOY504 transformants expressing the mutant pre-rRNA following growth for 6 h at 37°C. The effect of the mutation on cleavage at sites A0 and A1 was then analysed by primer extension. A dideoxynucleotide sequence ladder generated with the same primer was run alongside. Lane order in both panels is as described for Figure 3. (**A**) Primer extension from the oligonucleotide complementary to the 18S rRNA tag to A1. The position of the 18S rRNA tag, inserted at +190 with respect to the 5′-end of 18S rRNA, is represented by a square and cleavage site A1 is indicated by the arrow. (**B**) Primer extension from oligonucleotide 18S+34 to A0. The position of 18S+34, priming at nucleotide +34 with respect to the 5′-end of 18S rRNA, is indicated by a circle; cleavage site A0, 90 nt upstream of A1, is indicated by the arrow. The wild-type position of A0 cleavage of the plasmid-derived pre-rRNA can be seen in lane 1. A band 1 nt longer corresponds to residual cleavage of the chromosomally derived pre-rRNA (lane 2).

play a role in processing events at A1 are processing site A0, located 90 nt upstream (Hughes and Ares, 1991), and a site in the loop of the 3′-terminal stem–loop structure that was cross-linked *in vivo* to the U3 snoRNA (Beltrame and Tollervey, 1992). The role of A0 was assessed by substituting 6 nt across this site, yielding mutant A0sub6 (Figure 2B), while the importance of the loop structure was tested by deleting 18 nt from that region, including the cross-linked nucleotide (mutant ETSΔ18, schematically depicted in Figure 2B). Neither mutation was found to have any effect on either the steady-state level of 18S rRNA or the efficiency and accuracy of processing at A1 (data not shown). Interestingly, processing at A0 is also unaffected in these mutants. Neither the steady-state level of the pre-rRNA cleaved at A0 nor the position of cleavage is detectably affected, despite the fact that the nucleotides at the A0 cleavage site are altered by the A0sub6 mutation.

The secondary structure of the region around A0 and A1 is not well established, but will undoubtedly be changed by the substitution of 6 nt in the A0sub6 and A1-Xho mutations. Since alteration of the primary and secondary structure in the A1-Xho and -Sph mutants can be tolerated, we considered the possibility that the position of A1 was determined by a mechanism that measures the distance from some sequence or structure within the pre-rRNA to the actual processing site. As there are no other evidently conserved motifs in the 5′ ETS, we turned our attention to sequences within 18S rRNA itself. The local secondary and tertiary structure is very complex (Figure 2B), comprising three single-stranded nucleotides forming the 5′-end followed by the first stem–loop, which contains the universally conserved central pseudoknot (Gutell and Woese, 1990; Powers and Noller, 1991; Gutell *et al.*, 1994). This structure has been functionally implicated in translational accuracy, since mutations in this region, as well as in ribosomal proteins binding to this domain in *Escherichia coli*, lead to a *ram* (ribosomal ambiguity) phenotype (reviewed in Noller, 1991).

To assess whether spacing from one or more of these structures within 18S rRNA plays a role in determining the position of A1 three mutations were introduced which altered the spacing between A1 and the 5′ stem–loop in 18S rRNA by insertion of two or four uridines at position +3 (relative to the 5′-end of 18S rRNA) in the single-stranded region (Figure 2B, mutants A1+2U and A1+4U respectively) or by deletion of the AU dinucleotide (nucleotides +2 and +3) from this sequence (Figure 2B, mutant A1Δ2). None of these mutations prevents cell growth, as determined by plate assays, indicating that functional 18S rRNA is formed in all cases. Northern analysis indicated that the three mutations do not significantly influence the steady-state level of 18S rRNA (Figure 3, lanes 5–7). Primer extension analysis from the tag to A1, however, showed significant differences between the three mutants. In the A1+2U mutant the 5′-end of the 18S species is now heterogeneous (Figure 4A, lane 5). In addition to cleavage at the wild-type position (the upper band), a second cleavage occurs 2 nt downstream (lower

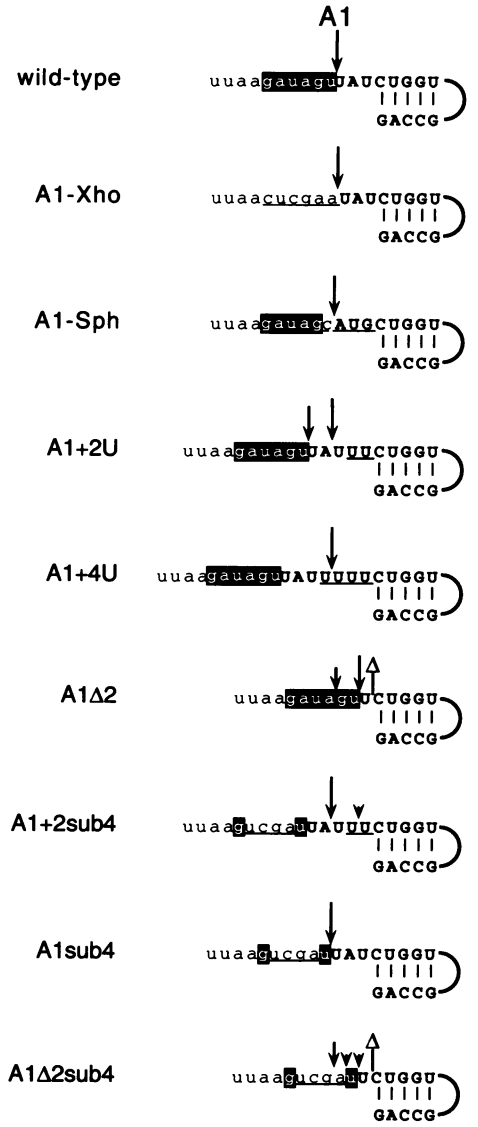

Fig. 5. Summary of the effect of mutations on cleavage at site A1. The diagram is a simplified version of the local primary and secondary structure with 5′ ETS nucleotides in lower case and 18S rRNA sequences in bold, upper case letters. The double-stranded structure corresponds to the 5′ helix in 18S rRNA, with the loop containing the pseudoknot drawn as a half-circle. The positions of the A1 cleavage site are indicated by the arrows. In the mutants which still possess the flanking phylogenetically conserved 6 nt these are shown in reverse contrast. Deviations from the wild-type sequence (substitutions or insertions) are underlined, while the Δ in mutants A1Δ2 and A1Δ2sub4 indicates the deletion of 2 nt from the 18S rRNA region. The size and location of the arrows in the different A1 mutants represents the efficiency and position of A1 cleavage.

band; see also Figure 5). When four uridines are inserted (A1+4U) only the lower 5′-end is observed (Figure 4A, lane 6) and the band corresponding to the normal cleavage position is absent. Upon deletion of 2 nt from this region (A1Δ2) heterogeneity is again observed for the 5′-end of the 18S rRNA, although the relative intensities of the bands differ (Figure 4A, lane 7). The lower band, representing cleavage at the wild-type position, is more intense than the upper band, originating from cleavage 2 nt upstream. These results show that in each mutant one rRNA species is observed with a 5′-end that is located 3 nt upstream from the base of the first stem–loop structure in 18S rRNA, irrespective of the nucleotide sequence at that position (see Figure 5, mutants A1+2U, A1+4U and A1Δ2). The fixed distance of A1 to the beginning of the 5′ stem–loop/pseudoknot structure therefore suggests that spacing is indeed one mechanism by which the site of processing at A1 is determined. In mutants A1+2U and A1Δ2 a second 5′-end is formed at a position such that it has the wild-type 5′ flanking sequence. In mutant A1+4U the insertion is apparently too large for this 5′-end to be formed. A second mechanism therefore appears to be operational that determines the cleavage site in a sequence-specific manner, most likely by making use of the conserved nucleotides around A1. In the wild-type situation both mechanisms define A1 cleavage at the same position, so inactivation of either mechanism would be masked by the continued functioning of the other.

To corroborate the existence of two partially independent mechanisms and the involvement of the upstream nucleotides two of the spacing mutations were combined with a substitution of the nucleotides upstream of A1, yielding mutants A1+2sub4 and A1Δ2sub4, with the A1sub4 mutation serving as a control for the effect of replacement alone (Figure 2B). In the single A1sub4 mutant and the A1+2sub4 mutant normal levels of 18S rRNA are detected (Figure 3, lanes 8 and 9), whereas the A1Δ2sub4 mutation significantly decreases the level of 18S rRNA (Figure 3, lane 10) and consequently results in a reduced growth rate at 37°C (data not shown). When the 5′-end of the 18S rRNA was analysed by primer extension mutant A1sub4 exhibited A1 cleavage at the normal site (Figure 4A, lane 9). This was expected in the light of the results obtained with the A1-Xho mutant. Interestingly, the A1+2sub4 mutant shows only one major 5′-end, corresponding to the cleavage that is 'spaced' 3 nt from the 5′ stem–loop (Figure 4A, lane 8). The second cleavage observed in the A1+2U mutant (the upper band in lane 5) is apparently abolished by substitution of the 4 nt upstream of A1, consistent with the hypothesis that they are important for the 'sequence recognition' mechanism (see also Figure 5). A minor additional band is observed 2 nt downstream. Similarly, the A1 cleavage observed at the wild-type position in the A1Δ2 mutant (Figure 4A, lane 7, lower band) is inhibited by the 4 nt substitution in A1Δ2sub4, but formation of the 5′-end 2 nt upstream is not affected (Figure 4A, lane 10). Some minor additional bands are also detected.

From these data we conclude that the site of processing at A1 can be specified by two distinct signals in the rRNA, i.e. recognition of the conserved nucleotides upstream of A1 in the 5′ ETS and a mechanism that determines cleavage at a fixed distance from the 5′ stem–loop/pseudoknot in 18S rRNA.

Pre-rRNA processing in A1 mutants

Since the introduction of the small mutations around A1 described above in some cases has a profound influence on the identity and efficiency of cleavage at this site, it was important to determine whether any other processing steps were affected. Furthermore, the fact that two redundant mechanisms appear to specify the position of the 5′-end of 18S rRNA raises the possibility that one of the mechanisms is obligatorily linked to specific additional processing steps. This is, for example, the case for

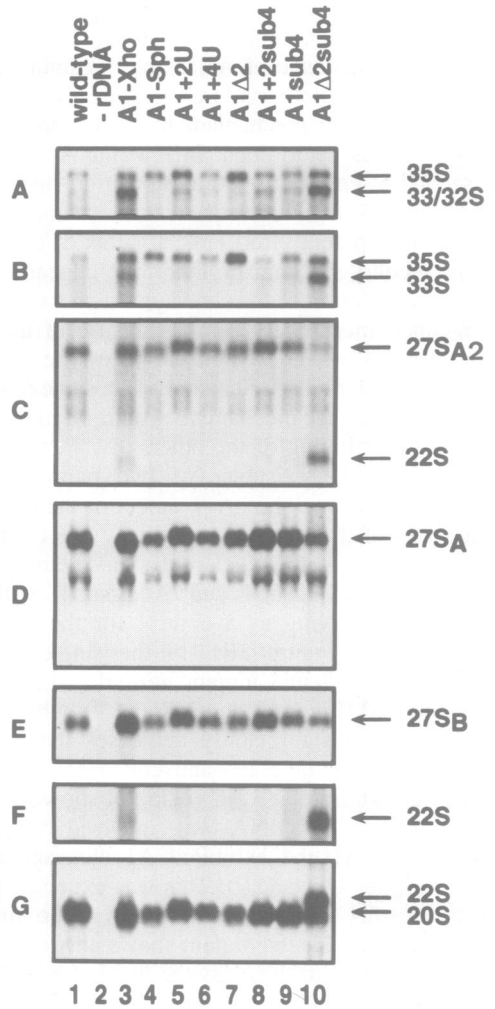

Fig. 6. Northern analysis of pre-rRNA processing in A1 mutants. RNA was extracted from NOY504 transformants expressing the mutant pre-rRNA following growth for 6 h at 37°C and analysed by Northern hybridization using oligonucleotides complementary to different regions of the transcribed spacers (see Figure 1 for their locations). The positions of the 35S, 33S, 32S, 27SA, 27SB and 20S pre-rRNAs, as well as that of the aberrant 22S species, are indicated on the right (see also Figure 1). For simplicity only relevant parts of each Northern blot are presented, which together show all pre-rRNA molecules detected in our experiments. The different panels are consecutive hybridizations of the same filter shown in Figure 3. Lane order is as in Figures 3 and 4. (**A** and **G**) Oligonucleotide 4, hybridizing in ITS1 upstream of A2. (**B** and **F**) Riboprobe 1, complementary to the A0→A1 fragment in the 5′ ETS. (**C**) Oligonucleotide 5, hybridizing in ITS1 between A2 and A3. (**D**) Oligonucleotide 6, hybridizing in ITS1 downstream of A3. (**E**) Oligonucleotide 7, hybridizing in ITS2. Oligonucleotide 5 (C) hybridizes specifically to $27SA_2$ pre-rRNA, while oligonucleotide 6 (D) hybridizes to both $27SA_2$ and $27SA_3$ pre-rRNA, which are not resolved.

processing at site A3 in ITS1, which is followed by exonucleolytic degradation to site $B1_S$, yielding the major short form of 5.8S rRNA in yeast (Henry *et al.*, 1994), while the minor long form of 5.8S rRNA is made by an alternative pathway involving processing at site $B1_L$.

In order to analyse processing in the A1 mutants Northern analysis was performed using oligonucleotide probes hybridizing to different regions in the transcribed spacers (see Figure 1 for their location). The panels in Figure 6 show the results obtained with the different probes for all A1 mutants. When comparing the positive and negative controls in lanes 1 and 2 respectively it is clear that the background hybridization due to Pol I transcribed pre-rRNA in the transformant carrying an 'empty' plasmid is negligible in all panels, indicating that in the mutants essentially all precursors are plasmid-derived, mutant molecules. Processing is not affected in the majority of the mutants, as judged from the normal relative amounts of all precursors in these transformants as compared with the wild-type control (Figure 6, cf. lanes 1 and 4–9), while aberrant precursors are detected in mutants A1-Xho and A1Δ2sub4 (lanes 3 and 10 in all panels). A moderate accumulation of 35S pre-rRNA is observed in the A1Δ2 mutant (Figure 6A and B, lane 7). In both the A1-Xho and the A1Δ2sub4 mutants a species designated 22S accumulates. This pre-rRNA is detected with oligonucleotide 4 located in ITS1 upstream of A2 (Figure 6G, lanes 3 and 10) and oligonucleotide 5 located between A2 and A3 in ITS1 (Figure 6C), but not with oligonucleotide 6 located downstream of A3 (Figure 6D). The 3′-end of the 22S species is therefore formed by processing at A3. The 22S pre-rRNA is also detected with a probe complementary to the 5′ ETS region between A1 and A0 (probe 1 in Figure 1) (Figure 6F, lanes 3 and 10). In addition, this probe reveals an increased level of a 33S species, extending from A0 to the 3′-end of the primary precursor, in the A1-Xho and A1Δ2sub4 mutants (Figure 6B). The 33S pre-rRNA is believed to be a normal intermediate in the processing pathway (see Figure 1), but it is undetectable by Northern hybridization in wild-type cells due to the rapid processing events at A1 and A2 following cleavage at A0. The increased level of the 33S pre-rRNA and accumulation of the aberrant 22S species observed in mutants A1Δ2sub4 and, to a lesser extent, A1-Xho is most probably due to a delay in processing at both A1 and A2. In the case of A1-Xho this effect is modest, which is also reflected in the otherwise normal amounts of the 20S and $27SA_2$ precursors, formed by cleavage of the 33S pre-rRNA at A2 (Figure 6C and G, lane 3), as well as that of the mature 18S rRNA (Figure 3, lane 3). In the A1Δ2sub4 mutant, however, accumulation is much more pronounced, leading to decreased steady-state levels of the $27SA_2$ precursor (Figure 6, panel C, lane 10) and mature 18S rRNA (Figure 3, lane 10).

The effect of the A1 mutations on processing at sites A2 and A3 was also assayed by primer extension from oligonucleotide 6 (see Figure 1). Both cleavages were accurate at the nucleotide level in all mutants. The steady-state levels of the pre-rRNAs cleaved at A2 and A3 were found to be normal in all cases, with the exception of the A1Δ2sub4 mutant, which exhibited a decreased signal originating from cleavage at the A2 site (data not shown). These results are in full agreement with the data obtained from the Northern analysis shown in Figure 6. Inhibition or reduction of either one of the mechanisms responsible for the positioning of A1 cleavage therefore does not appear to have any effect on the order of downstream processing events in the pathway. This indicates that neither A1 recognition mechanism is obligatorily coupled to a specific step at a later stage of pre-rRNA processing.

Since inactivation or reduction of either of the two mechanisms responsible for specifying the site of A1 processing does not result in a lethal phenotype, we considered the role of *trans*-acting factors that have been

shown to affect 18S rRNA synthesis but are nevertheless non-essential. Deletion of snR10 delays 18S rRNA maturation and leads to moderate accumulation of an aberrant 21S species, extending from A1 to A3, but does not influence the steady-state level of the mature rRNA (Tollervey, 1987). Genetic inactivation of the Nsr1p protein leads to cold sensitivity and decreases the steady-state level of 18S rRNA (Lee *et al.*, 1992). To assay for possible roles of these factors a representative collection of mutants (A1-Xho, A1-Sph, A1+2U and A1Δ2) was transformed into snr10$^-$ or nsr1$^-$ strains and analysed by Northern analysis for the steady-state level of 18S rRNA and by primer extension for A1 cleavage. Since these strains contain normal Pol I activity, it was not possible to specifically detect the steady-state levels of plasmid-derived pre-rRNA species. The results obtained were essentially identical to those obtained with the parental NOY504 strain (data not shown), making a specific function of snR10 or Nsr1p in either one of the recognition mechanisms at A1 unlikely.

Cleavage at A1 is endonucleolytic

Since the A0 cleavage site is located close to A1 in the proposed secondary structure, it was of interest to determine the possible effect of A1 mutations on processing at A0. Furthermore, it should, in principle, be possible to detect the 5′-end of the accumulated 33S pre-rRNA and the aberrant 22S species. The oligonucleotide complementary to the 18S rRNA tag is not extended very efficiently and is not useful for analysis of sites beyond A1 and we therefore used an oligonucleotide closer to the 5′-end of 18S rRNA (18S+34; see Figure 4B). There is a 1 nt polymorphism in the 3′-terminal region of the 5′ ETS between the chromosomal and the plasmid-encoded rDNA units. Hence, extension products terminating at site A0 on pre-rRNA derived from the GAL7–rDNA units are 1 nt shorter than those generated by primer extension on the chromosomal, Pol I-transcribed pre-rRNA (Beltrame *et al.*, 1994). This is seen in the wild-type transformant (Figure 4B, lane 1), which shows a band corresponding to the A0 cleavage that is 1 nt below that representing the residual cleavage observed in the negative control (Figure 4B, lane 2). In mutant A1-Xho the band at the A0 position is stronger, which could be expected in the light of the observed accumulation of the 33S and 22S species (Figure 4B, lane 3). This effect is much more pronounced in the A1Δ2sub4 mutant (Figure 4B, lane 10), in which case the band has also shifted down 2 nt in accordance with the deletion present in this mutant. All other mutants exhibit a normal level of A0 cleavage and in each case show the expected shift in the position of the band caused by deletion or insertion of nucleotides (Figure 4B, lanes 5–9). The A1-Sph mutation causes a severe reduction in cleavage at A0 (Figure 4B, lane 4); only cleavage at the position corresponding to residual chromosomal expression is detectable. These results show that in all cases processing at A0 occurs at the wild-type position and is therefore not influenced by a change in the position of A1 cleavage. Since A0 is detected from primers within 18S rRNA, this cleavage normally takes place (shortly) before A1.

If processing at A1 occurs by direct endonucleolytic cleavage it should be possible to detect the 5′ excised

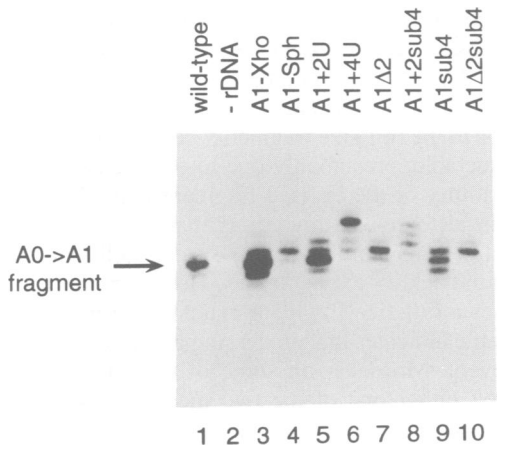

Fig. 7. Steady-state level of the A0→A1 fragment in A1 mutants. RNA was extracted from NOY504 transformants expressing the mutant pre-rRNA following growth for 6 h at 37°C. Samples were separated on a 10% polyacrylamide gel, transferred to a filter membrane and hybridized to a riboprobe complementary to the A0→A1 fragment (probe 1 in Figure 1). The position of the chromosomally derived fragment can be observed in lane 2 (–rDNA), although its abundance is variable in the different mutants. The size and/or the abundance of the plasmid-derived A0→A1 fragment in the A1 mutants varies depending on the particular mutation (see text). Lane order is identical to that in Figure 3.

product, i.e. the A0→A1 fragment, whereas this species will not be generated if A1 is formed by exonucleolytic digestion. To investigate this, total RNA was separated under conditions that resolved RNA species differing by a single nucleotide and a Northern blot prepared from this gel was hybridized to a riboprobe (1 in Figure 1) complementary to the 90 nt sequence from A0 to A1 (Figure 7). The wild-type transformant exhibits two fragments that differ by 1 nt in length (Figure 7, lane 1). The lower, more intense band is derived from the GAL7–rDNA units, since it is undetectable in the negative control (Figure 7, lane 2). The upper band represents the A0→A1 fragment derived from the chromosomal rDNA units and is detected at that position in all samples, although the intensity of this band is variable. In all A1 mutants plasmid-derived A0→A1 fragments are detectable whose sizes are in agreement with the observed positions of the A0 and A1 processing events (Figure 7, lanes 3–10). For example, the A1-Xho mutant exhibits an increased level of an A0→A1 fragment of the same size as the corresponding wild-type fragment (Figure 7, cf. lanes 1 and 3), in accordance with the wild-type positions of both the A0 and A1 cleavages (Figure 4, lane 3). In contrast, the A1-Sph mutant shows a strong decrease in the level of the A0→A1 fragment (Figure 7, lane 4), consistent with inhibition of A0 processing (Figure 4B, lane 4). The A1+4U transformant clearly shows one major fragment which is 4 nt longer than the wild-type (Figure 7, lane 6). In the A1+2U mutant two fragments can be detected, albeit with different intensity, which differ by 2 nt in length (Figure 7, lane 5), corresponding to the two 5′-ends of 18S rRNA observed in this mutant (Figure 4A, lane 5). In between these bands the chromosomally derived A0→A1 fragment, which is relatively intense in this case, can be observed.

The A0→A1 fragment, which contains only spacer

sequences, is a target for rapid exonucleolytic degradation, as is observed for spacer sequences in ITS1 (Stevens *et al.*, 1991; Henry *et al.*, 1994; D.Tollervey, unpublished results). This can be seen in Figure 7, where often, in addition to the full-size fragments, several smaller products are detectable, presumably due to exonucleolytic activity. The stability of the excised fragment may also not be the same in all cases, as mutations that alter the 3′-terminal nucleotides may influence the susceptibility of the fragment to attack by exonucleases. However, the fact that in all cases a full-size fragment extending from A0 to A1 is detectable indicates that processing at A1 is an endonucleolytic event. Moreover, in some of the mutants shown in Figure 7 either one of the two mechanisms determining A1 is presumed to be inactivated or at least much reduced. This is, for example, the case for the 'sequence recognition' mechanism in the A1-Xho and A1+4U mutants, whereas the 'spacing' mechanism is reduced in the A1Δ2 mutant. Despite this the A0→A1 fragment remains detectable in all cases, indicating that both mechanisms operate to define a site of endonucleolytic cleavage at A1.

Discussion

In this paper we have characterized in more detail the mechanism by which the 5′-end of yeast 18S rRNA (site A1) is specified and the signals in the pre-rRNA required for this. We introduced mutations surrounding the A1 cleavage site and analysed them in a genetic background where, under appropriate growth conditions, yeast cells temperature sensitive for Pol I transcription (Nogi *et al.*, 1993) can be rendered completely dependent upon synthesis and processing of mutant pre-rRNA (Henry *et al.*, 1994). Using this system we have found evidence for the existence of two mechanisms operating independently to define sites of endonucleolytic cleavage at A1.

It might have been expected that the nucleotide sequence across A1, as well as the phylogenetically conserved 6 nt immediately upstream, would be important for processing at this site. Substitution of these sequences in mutants A1-Xho and A1-Sph, however, had little affect on 18S rRNA synthesis and did not alter the position of cleavage, despite the fact that the nucleotides at the cleavage site are very different. These results argued against a role of the sequences around A1 in determining its position and suggested that this site was identified by measuring the distance from some structure in the pre-rRNA. The only other obvious candidate regions in the 5′ ETS, processing site A0 (90 nt upstream of A1) and a site of U3–5′ ETS *in vivo* cross-linking (45 nt upstream of A1), were shown not to be required for A1 cleavage. We therefore considered the possibility that sequences or structures within 18S rRNA were involved. When the distance between the A1 site and the 5′ stem–loop/pseudoknot structure in 18S rRNA region was varied (mutants A1+2U, A1+4U and A1Δ2) it was found that in each case a 5′-end was formed 3 nt from the base of the stem, strongly pointing towards the existence of a 'spacing' mechanism (Figure 5). Unexpectedly, however, the A1+2U and A1Δ2 mutants showed an additional 5′-end at a position that was flanked by the wild-type sequence. From this it was inferred that a second mechanism was also operating to define A1, which probably required the evolutionarily conserved sequence upstream of A1. This was substantiated by analysis of mutants in which substitution of four conserved upstream nucleotides was combined with alteration of the spacing within 18S rRNA (A1+2sub4 and A1Δ2sub4). Direct comparison of these mutants with their counterparts carrying only the altered spacing (A1+2U and A1Δ2 respectively) showed that substitution of the 4 nt selectively inhibited processing at the position of the wild-type sequence. The role of these nucleotides is normally masked and only becomes apparent when the 5′-end of 18S rRNA is heterogeneous. This could be the reason for the apparent lack of effect of substitution of the nucleotides surrounding A1 in mutants A1-Xho and A1-Sph. We therefore conclude that two mechanisms operate in parallel at the 5′-end of 18S RNA to define the A1 cleavage site. One mechanism acts by recognition of the phylogenetically conserved nucleotides in a sequence-specific manner, while the second mechanism operates from within 18S rRNA directing cleavage at a fixed distance of 3 nt from the 5′ stem–loop/pseudoknot structure. In the wild-type pre-rRNA both mechanisms specify the same site of cleavage.

The A1Δ2sub4 mutation reduces the efficiency of both mechanisms, thereby strongly delaying cleavage at A1. This is reflected in accumulation of the 33S pre-rRNA, arising from cleavage of the primary 35S precursor at A0, and of an aberrant 22S molecule, originating from cleavage of the 33S pre-rRNA at site A3 in ITS1 (Figure 6). The A1-Xho mutation also appears to delay A1 cleavage, but to a lesser extent. No such delay is observed for the A1sub4 mutant, which alters only the central nucleotides of the conserved 5′ flanking sequence. This may reflect the fact that the A1-Xho mutation also changes the nucleotide 5′ to the cleavage site. These results indicate that a delay in A1 cleavage results in inhibition of processing at A2 in ITS1. The fact that mutations *in cis* that block cleavage at A1 simultaneously affect A2 processing provides compelling evidence for the close coupling of both processing events. This was previously indicated by the observation that depletion of a number of *trans*-acting factors concomitantly blocks processing at A1 and A2 (Li *et al.*, 1990; Hughes and Ares, 1991; Morrissey and Tollervey, 1993; Beltrame *et al.*, 1994). In no case is a pre-rRNA detected which is cleaved at site A2 but not at A1, suggesting that A1 cleavage obligatorily precedes A2 cleavage.

In contrast to the coupling between A1 and A2, processing at A0 and A1 does not appear to be obligatorily coupled. The A1-Sph mutation strongly inhibits processing at A0 with little effect at A1, showing that A0 processing need not precede cleavage at A1. Moreover, alteration of the efficiency and/or position of cleavage at A1 does not simultaneously affect A0, since cleavage at A0 is observed at the wild-type position in all mutants. The reason for the severe reduction at A0 in the A1-Sph mutant remains unclear. In the proposed secondary structure model for the 5′ ETS both sites are in close proximity to each other (see Figure 2B), but the substitutions in A1-Sph are not predicted to affect the local structure at A0. In striking contrast to the effects of the A1-Sph mutation, the A0sub6 mutation does not detectably affect the position or efficiency of A0 processing. The mechanism of A0 cleavage and its role in the pre-rRNA processing pathway therefore remain unclear. It is clear that with either

mechanism A1 is formed by an endonucleolytic activity, as shown by the fact that in all mutants the full-length A0→A1 fragment is detectable.

The exact nature of the sequences or structures within 18S rRNA involved in the spacing mechanism remains to be determined. Due to their proximity to the cleavage site, the 5′ 3 nt were obvious candidates, but their identity is not essential for cleavage (cf. mutants A1Δ2, A1+2U and A1+2sub4). However, it is possible that certain nucleotides are preferred over others, which may explain the lower processing rate in the A1Δ2/A1Δ2sub4 mutants, where cleavage takes place 5′ to a purine (G and A respectively), in comparison with the A1+2U/A1+4U/A1sub4 mutants, where in each case, as in the wild-type, cleavage occurs 5′ to a U residue. Its location 5′ to an A may also explain the decreased efficiency of A1 cleavage in the A1-Sph mutant, although in this case the sequence recognition system specifies cleavage at the same site. The 5′ helix, together with the loop closing it, containing the universally conserved pseudoknot, may also play a role in a mechanism operating from within 18S rRNA. Interestingly, a substitution mutation was recently identified in the corresponding stem–loop in 16S rRNA of *E.coli* that causes cold sensitivity (Dammel and Noller, 1993). This C23→U transition, which is predicted to destabilize the 5′ helix, impairs ribosome assembly and function and in addition affects maturation of the 5′-end of 16S rRNA. In this organism an alternative secondary structure can be drawn that consists of upstream leader nucleotides base paired with nucleotides of 16S rRNA which in the mature ribosome form the 5′ helix and pseudoknot. A similar structure can be drawn for yeast 18S rRNA and 5′ ETS sequences, but not for higher eukaryotes.

The results presented in this paper indicate that the exact site of A1 cleavage is determined by making use of two distinct signals in the pre-rRNA. It is less clear whether the cleavages specified by the different mechanisms also represent two processing systems, as is the case for the 5′-ends of 5.8S rRNA (Henry *et al.*, 1994). It is also possible that one processing system responds to two different sets of signals, which would be more similar to the situation observed in pre-mRNA splicing (reviewed in Madhani and Guthrie, 1994). Interactions between the terminal regions of the 5′ exon–intron boundary with U1 snRNP initially establish the region as a 5′ splice site. Subsequently the site of cleavage is specified by interactions of sequences both 5′ and 3′ to the actual splice site with the U5 and U6 snRNPs respectively. A similar role might be played by a large, multi-RNP complex responsible for cleavages at sites A1 and A2 (see Morrissey and Tollervey, 1995). These cleavages require the essential snoRNAs U3, U14 and snR30 (Li *et al.*, 1990; Hughes and Ares, 1991; Morrissey and Tollervey, 1993) and their associated proteins Nop1p, Sof1p and Gar1p (Tollervey *et al.*, 1991; Girard *et al.*, 1992; Jansen *et al.*, 1993). In the case of U3 the evolutionarily well-conserved box A sequence displays perfect complementarity to nucleotides that in the mature ribosome form the 5′ helix and the pseudoknot structure (J.M.X.Hughes, personal communication). Furthermore, 4 nt in this region of the U3 snoRNA could be specifically cross-linked to 35S rRNA, although the location of the cross-linked nucleotides in the rRNA was not determined (Beltrame and Tollervey, 1992). The U3–18S rRNA interaction therefore is a likely candidate to play a direct role in processing at A1. The role of two non-essential factors previously shown to be involved in 18S rRNA synthesis, snR10 and Nsr1p (Tollervey, 1987; Lee *et al.*, 1992), was tested by analysing four A1 mutants in strains deleted for these genes. Since no differences were found when the same mutations were expressed in the parental strain, a specific role of these factors in either mechanism specifying the site of A1 cleavage is very unlikely.

The presence of several redundant pathways leading to mature rRNAs can be advantageous for the cell in maintaining efficient synthesis of ribosomal RNA and thus of ribosomes. The existence of multiple processing routes may provide a means of regulating pre-rRNA processing and therefore ribosome biogenesis in general under different physiological conditions. Alternatively, different pathways may act as 'fail-safe' mechanisms to ensure correct and efficient ribosome synthesis.

Materials and methods

Strains and media

Growth and handling of *S.cerevisiae* was performed by standard techniques. For all experiments shown the yeast strain used was NOY504: MATα; *rrn4::LEU2*; *leu2-3, 112*; *ura3-1*; *trp1-1*; *his3-11*; *CAN1-100* (Nogi *et al.*, 1993; generously provided by Dr M.Nomura, UCI, Irvine, CA). This strain carries a disrupted *rrn4* (*rpa12*) gene, resulting in a temperature-sensitive phenotype due to inactivation of RNA polymerase I. The *nsr1*$^-$ strain (generously provided by Dr T.Mélèse, Columbia University, New York, NY) was WLY353: MATa; *nsr1::HIS3*; *ade2-1*; *his3-11,15*; *leu2-3,112*; *trp1-1*; *ura3-1; CAN1-100* (Lee *et al.*, 1992). The *snr10*$^-$ strain was D111: MATa; *snr10::LEU2*; *ade2-101*; *his3-Δ*; *leu2-3,112*; *trp1-Δ*; *ura3-52*.

Plasmids and construction of mutations

The wild-type rDNA plasmid was pGAL::rDNA (Henry *et al.*, 1994), carrying the entire yeast rDNA unit fused to the *GAL7* promoter (Nogi *et al.*, 1991) in YEp24 (2μm-URA3). It further contains small oligonucleotide insertions (tags) in the 18S, 5.8S and 25S rRNA genes. The plasmid used as a negative control (–rDNA) was YEplac195 (2μm-URA3) (Gietz and Sugino, 1988). For subcloning fragments containing A1 mutations plasmid pTH66 was used, which contains a 1 kb *Bam*HI fragment, consisting of the *GAL7* promoter, the 5′ ETS and 18S rRNA sequences up to the *Bam*HI site in the 18S rRNA tag, cloned into pBluescript-KS(+). All mutations were produced by a two-step PCR procedure. In the first round the mutagenic primer was used in combination with a primer complementary to sequences in the 5′ ETS, after which the gel-purified PCR product was combined with a downstream primer in the 18S region to yield the final PCR product. From this a 200 bp *Hin*dIII–*Nde*I fragment (containing the region around A1) was subcloned into pTH66 and fully sequenced. Correct clones were then used to exchange the 1 kb *Bam*HI fragment from pGAL::rDNA for the one carrying the A1 mutation. The presence of the mutation in the pGAL::rDNA plasmid was certified by sequencing of the A1 region.

Northern hybridization

Yeast cells transformed with wild-type or mutant plasmids were grown in 50 ml cultures of liquid synthetic galactose medium at 25°C until mid-log phase and then diluted to an OD_{600} of 0.09 and shifted for 6 h to 37°C (Henry *et al.*, 1994). Total RNA was extracted, separated on 1.2% agarose–formaldehyde gels and transferred to Hybond N^+ membranes as described (Tollervey, 1987). For separation of low molecular weight RNA samples were run on a 40 cm long, 10% polyacrylamide gel in 1× TBE buffer until the xylene cyanol dye marker reached the bottom of the gel. Gels were then stained with ethidium bromide, photographed and electroblotted in 0.5× TBE onto Hybond N^+ according to standard procedures. Aliquots of 5 μg RNA were used for each sample for both gel types. Northern blots were hybridized as described previously with the following oligonucleotides (see Figure

1): (2, 18S tag) 5′-CGAGGATCCAGGCTTT-3′; (3, 25S tag) 5′-ACTCGAGAGCTTCAGTAC-3′; (4) 5′-GCTCTTTGCTCTTGCC-3′; (5) 5′-TGTTACCTCTGGGCCC-3′; (6) 5′-CCAGTTACGAAAATT-CTTG-3′; (7) 5′-GGCCAGCAATTTCAAGTTA-3′. Furthermore, a riboprobe overlapping the A0→A1 fragment was used (probe 1 in Figure 1). For this a 115 bp fragment extending from the 5′-end of the 18S rRNA gene (A1) up to the *Pvu*II site 25 nt upstream of A0 in the 5′ ETS was generated by PCR and cloned into pBluescript KS(+). The plasmid was linearized with *Pvu*II and labelled RNA was synthesized *in vitro* using [^{32}P]UTP and T3 RNA polymerase according to standard procedures.

Primer extension

Primer extension was performed as described previously (Beltrame and Tollervey, 1992) using 5 μg total RNA. The primers used were the 18S tag and (18S+34) 5′-CATGGCTTAATCTTTGAGAC-3′. Sequences run alongside the primer extension were generated using the same oligonucleotide phosphorylated with unlabelled ATP.

Acknowledgements

We thank Drs M.Nomura (UCI, Irvine, CA) and T.Mélèse (Columbia University, New York, NY) for the generous gift of yeast strains. We thank Bertrand Séraphin, Zoi Lygerou and Iain Mattaj and all the members of our laboratory for critical reading of the manuscript. J.V. was supported by a long-term fellowship from the European Molecular Biology Organization (EMBO). Y.H. was supported by a grant from the European Molecular Biology Laboratory (EMBL).

References

Apirion,D. and Miczak,A. (1993) RNA processing in prokaryotic cells. *BioEssays*, **15**, 113–120.

Balzi,E., Di Pietro,A., Goffeau,A., Van Heerikhuizen,H. and Klootwijk,J. (1985) The RNA polymerase I initiation site and the external transcribed spacer of the fission yeast *Schizosaccharomyces pombe* ribosomal RNA genes. *Gene*, **39**, 165–172.

Beltrame,M. and Tollervey,D. (1992) Identification and functional analysis of two U3 binding sites on yeast pre-ribosomal RNA. *EMBO J.*, **11**, 1531–1542.

Beltrame,M., Henry,Y. and Tollervey,D. (1994) Mutational analysis of an essential binding site for the U3 snoRNA in the 5′ external transcribed spacer of yeast pre-rRNA. *Nucleic Acids Res.*, **22**, 5139–5147.

Dammel,C.S. and Noller,H.F. (1993) A cold-sensitive mutation in 16S rRNA provides evidence for helical switching in ribosome assembly. *Genes Dev.*, **7**, 660–670.

Eichler,D.C. and Craig,N. (1994) Processing of eukaryotic ribosomal RNA. *Prog. Nucleic Acid Res. Mol. Biol.*, **49**, 197–239.

Gietz,R.D. and Sugino,A. (1988) New yeast–*Escherichia coli* shuttle vectors constructed with *in vitro* mutagenized yeast genes lacking six-base pair restriction sites. *Gene*, **74**, 527–534.

Girard,J.P., Lehtonen,H., Caizergues-Ferrer,M., Amalric,F., Tollervey,D. and Lapeyre,B. (1992) GAR1 is an essential small nucleolar RNP protein required for pre-rRNA processing in yeast. *EMBO J.*, **11**, 673–682.

Gutell,R.R. and Woese,C.R. (1990) Higher order structural elements in ribosomal RNAs: pseudo-knots and the use of non-canonical pairs. *Proc. Natl Acad. Sci. USA*, **87**, 663–667.

Gutell,R.R., Larsen,N. and Woese,C.R. (1994) Lessons from an evolving rRNA: 16S and 23S rRNA structures from a comparative perspective. *Microbiol. Rev.*, **58**, 10–26.

Hannon,G.J., Maroney,P.A., Branch,A., Benenfield,B.J., Robertson,H.D. and Nilsen,T.W. (1989) Accurate processing of human pre-rRNA *in vitro*. *Mol. Cell. Biol.*, **9**, 4422–4431.

Henry,Y., Wood,H., Morrissey,J.P., Petfalski,E., Kearsey,S. and Tollervey,D. (1994) The 5′ end of yeast 5.8S rRNA is generated by exonucleases from an upstream cleavage site. *EMBO J.*, **13**, 2452–2463.

Hughes,J.M.X. and Ares,M.J. (1991) Depletion of U3 small nucleolar RNA inhibits cleavage in the 5′ external transcribed spacer of yeast pre-ribosomal RNA and impairs formation of 18S ribosomal RNA. *EMBO J.*, **10**, 4231–4239.

Jansen,R., Tollervey,D. and Hurt,E.C. (1993) A U3 snoRNP protein with homology to splicing factor PRP4 and Gb domains is required for ribosomal RNA processing. *EMBO J.*, **12**, 2549–2558.

Kass,S., Tyc,K., Steitz,J.A. and Sollner-Webb,B. (1990) The U3 small nuclear ribonucleoprotein functions at the first step of preribosomal RNA processing. *Cell*, **60**, 897–908.

Klootwijk,J. and Planta,R.J. (1989) Isolation and characterization of yeast ribosomal RNA precursors and preribosomes. *Methods Enzymol.*, **180**, 96–109.

Lafontaine,D., Vandenhaute,J. and Tollervey,D. (1995) The 18S rRNA dimethylase Dim1p is required for pre-ribosomal RNA processing in yeast. *Genes Dev.*, in press.

Lee,W.-C., Zabetakis,D. and Mélèse,T. (1992) NSR1 is required for pre-rRNA processing and for the proper maintenance of steady-state levels of ribosomal subunits. *Mol. Cell. Biol.*, **12**, 3865–3871.

Li,H.V., Zagorski,J. and Fournier,M.J. (1990) Depletion of U14 small nuclear RNA (snR128) disrupts production of 18S rRNA in *Saccharomyces cerevisiae*. *Mol. Cell. Biol.*, **10**, 1145–1152.

Madhani,H.D. and Guthrie,C. (1994) Dynamic RNA–RNA interactions in the spliceosome. *Annu. Rev. Genet.*, **28**, 1–26.

Morrissey,J.P. and Tollervey,D. (1993) Yeast snR30 is a small nucleolar RNA required for 18S rRNA synthesis. *Mol. Cell. Biol.*, **13**, 2469–2477.

Morrissey,J.P. and Tollervey,D. (1995) Birth of the snoRNPs—the evolution of RNase MRP and the eukaryotic pre-rRNA processing system. *Trends Biochem. Sci.*, **20**, 78–82.

Mougey,E.B., Pape,L.K. and Sollner-Webb,B. (1993) A U3 small nucleolar ribonucleoprotein-requiring processing event in the 5′ external transcribed spacer of *Xenopus* precursor rRNA. *Mol. Cell. Biol.*, **13**, 5990–5998.

Nogi,Y., Yano,R. and Nomura,M. (1991) Synthesis of large rRNAs by RNA polymerase II in mutants defective in RNA polymerase I. *Proc. Natl Acad. Sci. USA*, **88**, 3962–3966.

Nogi,Y., Yano,R., Dodd,J., Carles,C. and Nomura,M. (1993) Gene *RRN4* in *Saccharomyces cerevisiae* encodes the A12.2 subunit of RNA polymerase I and is essential only at high temperatures. *Mol. Cell. Biol.*, **13**, 114–122.

Noller,H.F. (1991) Ribosomal RNA and translation. *Annu. Rev. Biochem.*, **60**, 191–227.

Powers,T. and Noller,H.F. (1991) A functional pseudoknot in 16S ribosomal RNA. *EMBO J.*, **10**, 2203–2214.

Srivastava,A.K. and Schlessinger,D. (1990) Mechanism and regulation of bacterial ribosomal RNA processing. *Annu. Rev. Microbiol.*, **44**, 105–129.

Stevens,A., Hsu,C.L., Isham,K.R. and Larimer,F.W. (1991) Fragments of the internal transcribed spacer 1 of pre-rRNA accumulate in *Saccharomyces cerevisiae* lacking 5′→3′ exoribonuclease 1. *J. Bacteriol.*, **173**, 7024–7028.

Tollervey,D. (1987) A yeast small nuclear RNA is required for normal processing of pre-ribosomal RNA. *EMBO J.*, **6**, 4169–4175.

Tollervey,D., Lehtonen,H., Carmo-Fonseca,M. and Hurt,E.C. (1991) The small nucleolar RNP protein NOP1 (fibrillarin) is required for pre-rRNA processing in yeast. *EMBO J.*, **10**, 573–583.

Udem,S.A. and Warner,J.R. (1973) The cytoplasmic maturation of a ribosomal precursor ribonucleic acid in yeast. *J. Biol. Chem.*, **248**, 1412–1416.

Van Nues,R.W., Venema,J., Rientjes,J.M.J., Dirks-Mulder,A. and Raué,H.A. (1995) Processing of eukaryotic pre-rRNA: the role of the transcribed spacers. *Biochem. Cell Biol.*, in press.

Veldman,G.M., Brand,R.C., Klootwijk,J. and Planta,R.J. (1980) Some characteristics of processing sites in ribosomal precursor RNA of yeast. *Nucleic Acids Res.*, **8**, 2907–2920.

Yeh,L.-C.C. and Lee,J.C. (1992) Structure analysis of the 5′ external transcribed spacer of the precursor ribosomal RNA from *Saccharomyces cerevisiae*. *J. Mol. Biol.*, **228**, 827–839.

Yu,Y.-T. and Nilsen,T.W. (1992) Sequence requirements for maturation of the 5′ terminus of human 18S rRNA *in vitro*. *J. Biol. Chem.*, **267**, 9264–9268.

Received on June 12, 1995; revised on July 12, 1995